

Particle Size Measurements Using Data from a High Spectral Resolution Lidar and a Millimeter Wavelength Radar

E. Eloranta, J. Garcia, I. Razenkov and J. Hedrick
1225 W. Dayton St
University of Wisconsin-Madison
eloranta@lidar.ssec.wisc.edu

The University of Wisconsin Arctic High Spectral Resolution Lidar (AHSRL) and the ARM 8.6 mm radar (MMCR) collected data during the Mixed-Phase Cloud Experiment (M-PACE). The AHSRL provides measurements of the backscatter cross section, extinction cross section, and depolarization that are robustly calibrated by reference to molecular scattering. In addition, the AHSRL receiver accepts light from a very small angular field-of-view (45 microradian) limiting errors caused by multiply scattered photons. These factors make AHSRL data uniquely suited for use in lidar-radar particle size retrievals. This paper presents examples of lidar-radar particle size retrievals, compares derived precipitation estimates with conventional meteorological measurements and looks at the use of fall velocities to provide particle shape information.

Our size retrieval follows that of Donovan and Lammeren (JGR, V106, D21, p 27425). The lidar and radar backscatter cross sections are used to derive:

$$D_{\text{eff prime}} = \left(\frac{9}{\pi} \frac{\langle \text{Volume}^2 \rangle}{\langle \text{Area} \rangle} \right)^{1/4} \quad \text{where } \langle \rangle \text{ denotes an average over the particle size distribution.}$$

$$D_{\text{eff prime}} \sim \left(\frac{\text{Radar backscatter cross section}}{\text{Lidar scattering cross section}} \right)^{1/4}$$

We can use either the lidar backscatter cross section or the directly measured extinction cross section in this retrieval. Typically, we use the backscatter cross section and an assumed value of the backscatter phase function (.035) to compute the lidar scattering cross section. The AHSRL backscatter cross section measurement is not affected by multiple scattering errors and it is less affected by measurement noise.

$D_{\text{eff prime}}$ is easily measured with little potential error due to a priori assumptions. However, determination of liquid water content, and number density require measurements of the effective diameter:

$$D_{\text{eff}} = \frac{3}{2} \frac{\langle \text{Volume} \rangle}{\langle \text{Area} \rangle}$$

In regions where the lidar measures depolarizations of less than 3%, we assume that the scattering particles are spherical. In this case we assume a modified gamma distribution of particle sizes, $N(D)$:

$$N(D) = aD^\alpha \exp(-bD^\gamma)$$

Given assumed values for the dispersion parameters α and γ , The measured lidar cross section and the computed $D_{\text{eff prime}}$ values are used to solve for the values of a and b . $N(D)$ is then used to compute the relationship between $\langle \text{Volume}^2 \rangle$ and $\langle \text{Volume} \rangle$ allowing us to convert from $D_{\text{eff prime}}$ to D_{eff} .

In the case of ice particles the conversion of $D_{\text{eff prime}}$ to D_{eff} is made more difficult by the wide variety of crystal shapes present in cirrus clouds and falling snow. When the measured lidar depolarization is greater than 3%, we assume the particles are ice crystals. We allow the specification of separate dispersion parameters for the gamma distribution of water droplets and of ice crystal sizes. In addition, we assume power law relationships describing the projected area and volume of crystals as a function of the crystal diameter (the longest axis of the particle). This approach is described by a number of authors including Mitchell (JAS, V 53, 1996, p 1710). Rewriting Mitchell's power law relationships slightly in order to make the coefficients non-dimensional:

$$\text{Area} = \sigma_a \frac{\pi}{4} D_r^2 \left(\frac{D}{D_r} \right)^{\delta_a}$$

$$\text{Volume} = \sigma_v \frac{\pi}{6} D_r^3 \left(\frac{D}{D_r} \right)^{\delta_v}$$

Where σ_v is the fraction of the volume of the sphere with a diameter of D_r that is filled with ice and σ_a is the fraction of the projected area of a sphere with diameter D_r that is covered by ice. The coefficients δ_a and δ_v can be specified separately for particles smaller than and larger than the reference diameter D_r .

This particle size retrieval has been incorporated into our web page 'http://lidar.ssec.wisc.edu' and can be applied to any of the lidar and radar data collected during M-PACE or the data that has been collected at Eureka, Canada since August of 2005. All data is provided in the form of netCDF files which can be downloaded by anyone. The user can specify the time and altitude interval, the time and altitude averaging and all of the assumed parameters needed for size, number density and liquid water retrievals. A reproduction of the web page providing access to this data is shown below.

To generate a Downloadable NetCDF Dataset, select UTC time and averaging intervals for data

From: year 2006 month December day 11 hour 15 minute 45
To: year 2006 month December day 11 hour 17 minute 45

Min altitude: 0 km Time Resolution: 30 seconds/record
Max altitude: 15 km Altitude Resolution: 30 meters/point

Continuous Time Axis
 Minimum Signal to Noise Ratio

[Documentation](#)

under construction

Select your desired datasets:

Derived Quantities	Raw Data	Radar Quantities (MMCR)
<input checked="" type="checkbox"/> Particulate Backscatter Cross Section	<input checked="" type="checkbox"/> Combined Channel Counts	<input checked="" type="checkbox"/> Reflectivity
<input checked="" type="checkbox"/> Particulate Optical Depth	<input checked="" type="checkbox"/> Molecular Channel Counts	<input checked="" type="checkbox"/> Backscatter Cross Section
<input checked="" type="checkbox"/> Particulate Depolarization	<input checked="" type="checkbox"/> Cross Polarized Channel Counts	<input checked="" type="checkbox"/> Spectral Width
<input checked="" type="checkbox"/> Particulate Extinction Cross Section	<input checked="" type="checkbox"/> Radiosonde Profile(s)	<input checked="" type="checkbox"/> Doppler Velocity
<input checked="" type="checkbox"/> Attenuated Molecular Backscatter	<input checked="" type="checkbox"/> Molecular Scattering Cross Section	
<input checked="" type="checkbox"/> Error Estimates	<input checked="" type="checkbox"/> Calibration/System Measurements	
	<input checked="" type="checkbox"/> Data Quality Metrics (incomplete)	
AERI Quantities	Micro-wave Radiometer Quantities	HSRL/MMCR Cooperative Quantities
<input checked="" type="checkbox"/> Brightness Temperature	<input checked="" type="checkbox"/> Brightness Temperature	<input checked="" type="checkbox"/> Effective Diameter Prime
<input checked="" type="checkbox"/> Variability	<input checked="" type="checkbox"/> Water Path	<input checked="" type="checkbox"/> Particle Measurements

[Particle Size Distribution Parameters](#)

New Code. Use with caution
Check your Distribution Graphs.

Size Distribution Graphs

$n(D) = aD^\alpha \exp(-bD^\gamma)$

Water: $\alpha = 2$ $\gamma = 1$ Ice: $\alpha = 1$ $\gamma = 1$

Ice:

Ice Crystal Type Preset: Bullet Rosettes (Mitchell 1996)

$A = \sigma_a \frac{\pi}{4} D_r^2 \left(\frac{D}{D_r} \right)^{\delta_a}$ $V = \sigma_v \frac{\pi}{6} D_r^3 \left(\frac{D}{D_r} \right)^{\delta_v}$

$D_r = 60$ microns $\sigma_a = 1.0$ $\sigma_v = 0.26$

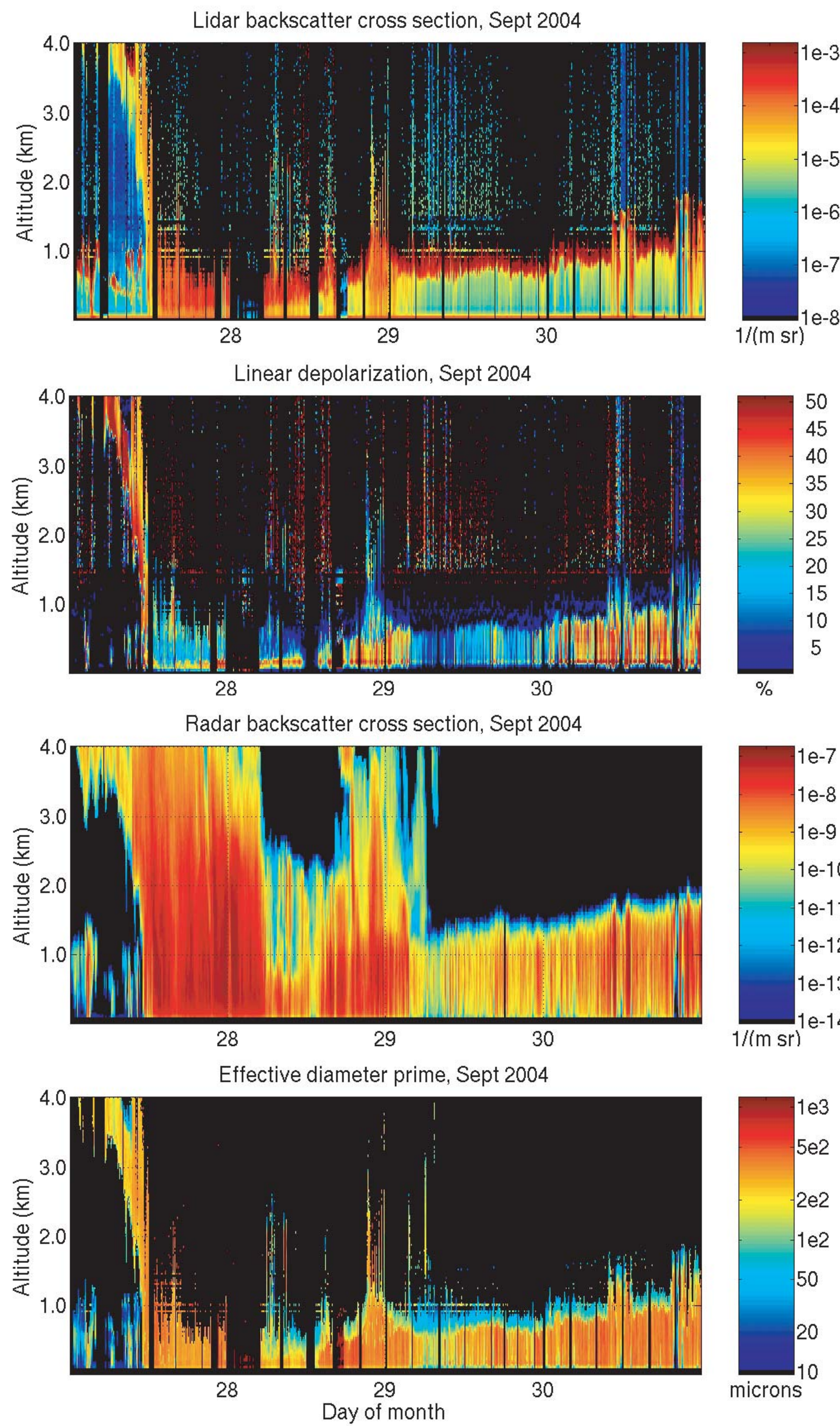
$D < D_r$: $\delta_a = 2$ $\delta_v = 3$

$D \geq D_r$: $\delta_a = 1.57$ $\delta_v = 2.26$

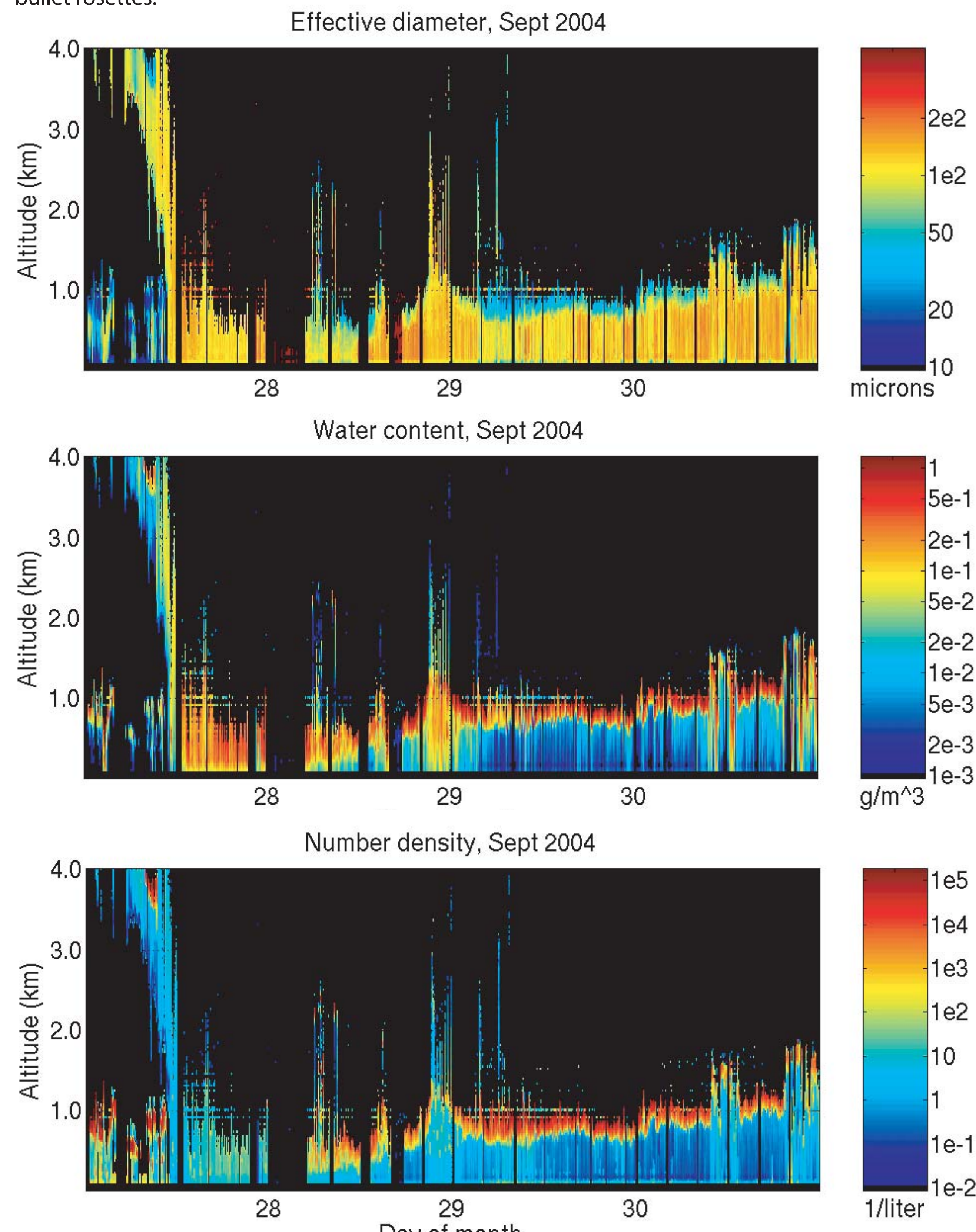
[Backscatter Phase Function used for Effective Diameter Prime](#)

Ice: $\frac{P(180)}{4\pi} = 0.035 \frac{1}{sr}$

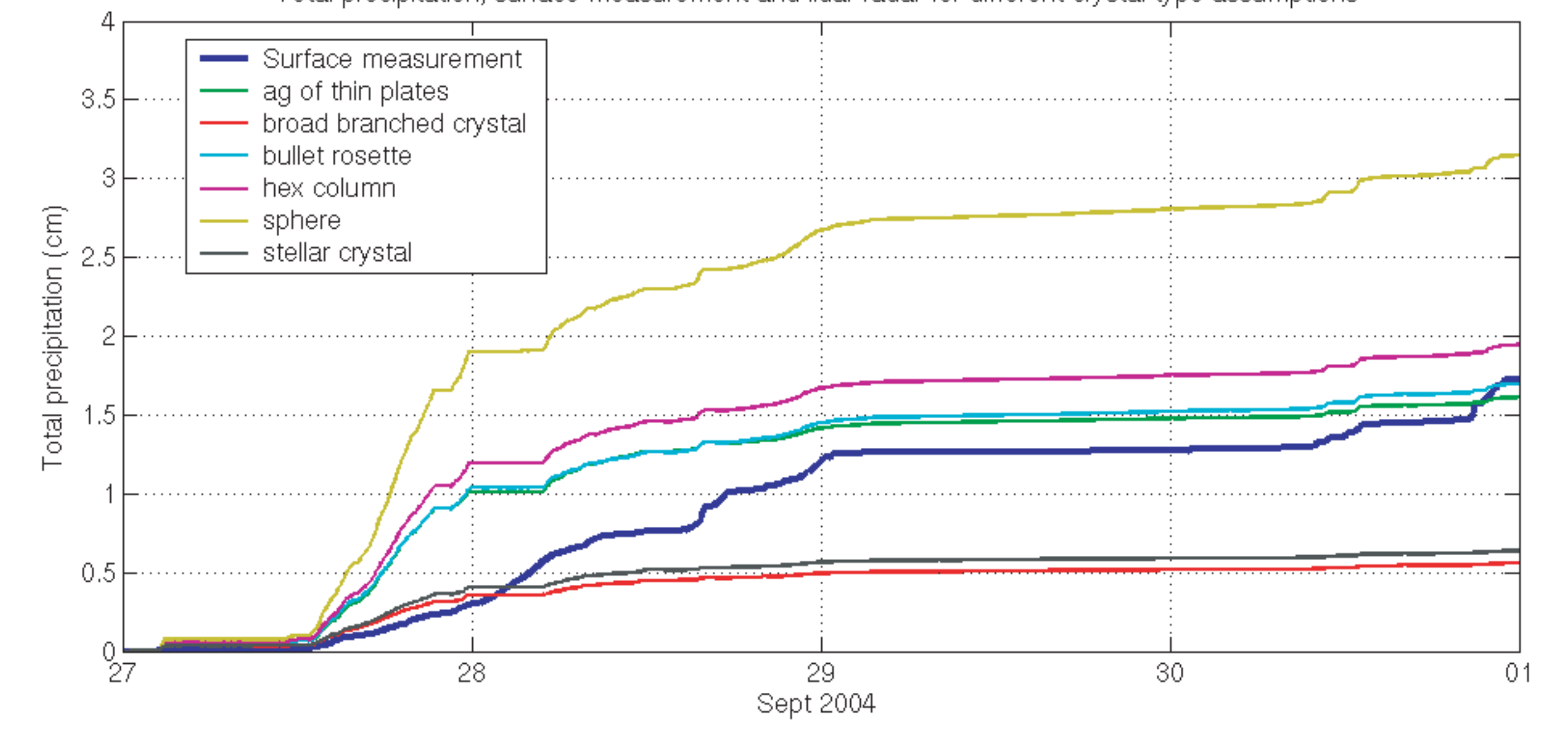
Particle size measurements in the form of effective diameter prime are derived for M-PACE data acquired between Sept 27 and Oct 1. Lidar and radar data are shown along the the derived particle size.



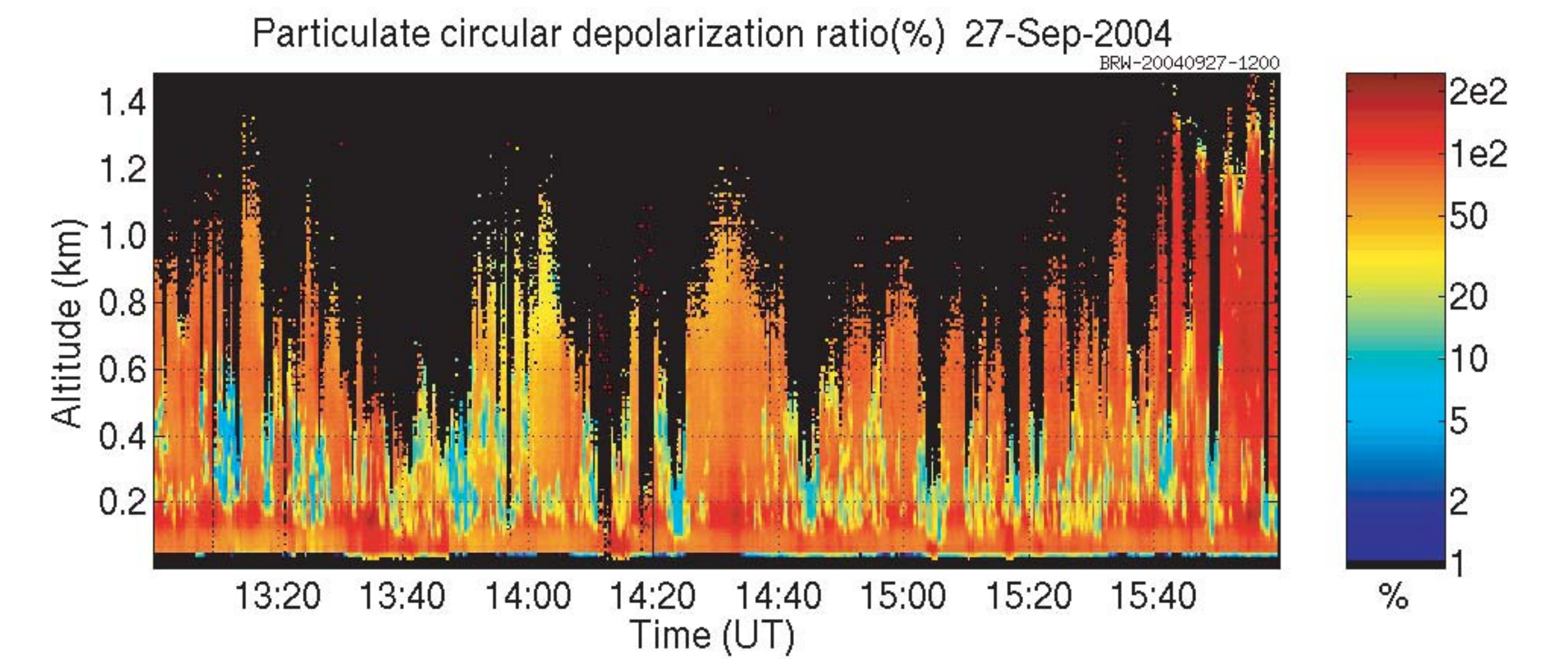
Conversion of 'effective diameter prime' to 'effective diameter' and derivation of water content or number density requires use of an assumed particle size distribution for water clouds and both an assumed size distribution and a crystal type for ice clouds. The following assume gamma distribution parameters $\alpha=2, \gamma=1$ for water and $\alpha=1, \gamma=1$ for ice. Ice crystals are assumed to be bullet rosettes.



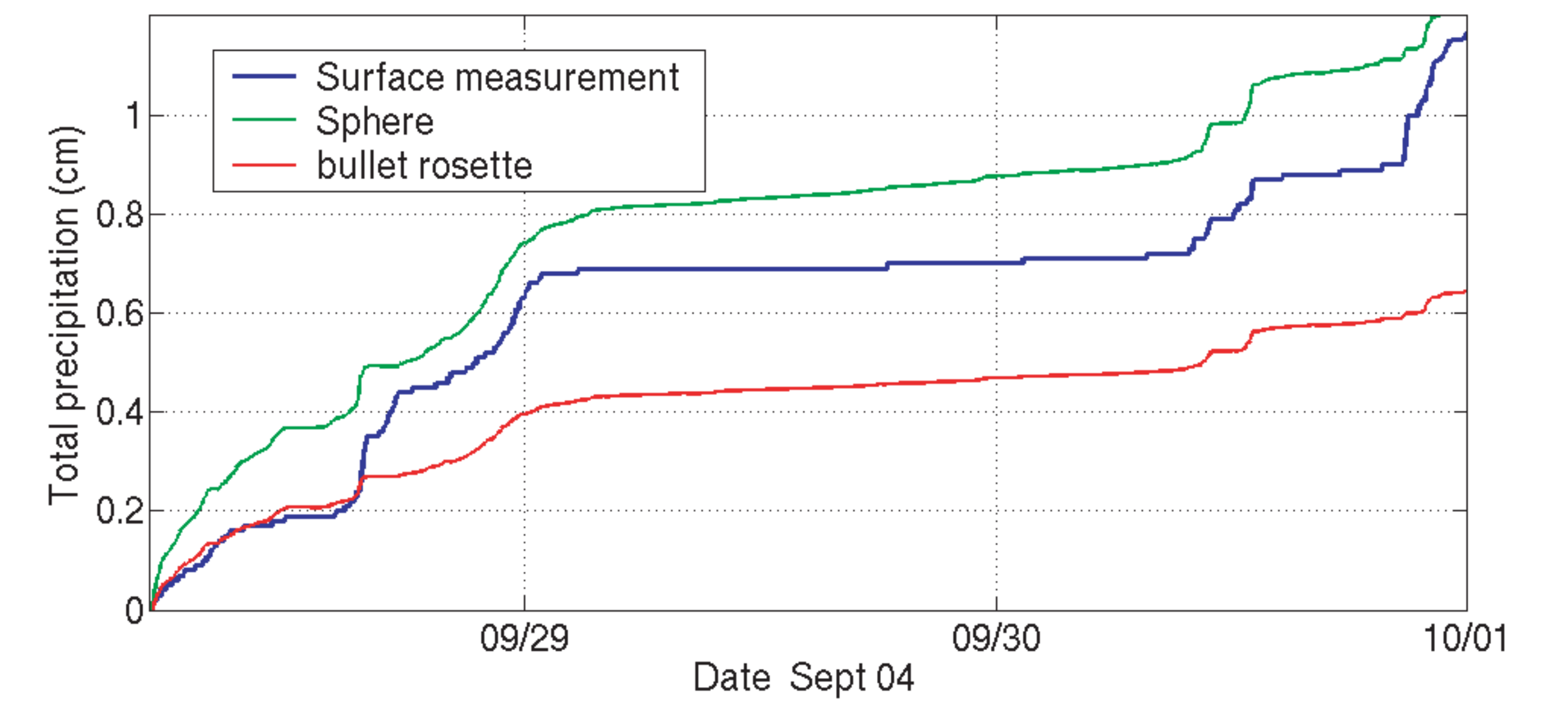
The vertical flux of water can be computed using the radar measured vertical velocity and the lidar-radar derived water content. The flux of water computed an altitude of 250 m using several crystal type assumptions is compared with surface measurements of precipitation in the next figure.



The surface measurement (blue) shows a slower accumulation rate than all of the model results on Sept 27. An examination of the lidar depolarization data for this period shows that water clouds embedded in the snowfall increase the water content at 250 m. It appears that the over prediction of the precip rate results because the radar velocity is highly weighted towards the falling snow and thus the flux is computed assuming that the cloud water is falling at the same velocity as the snow.

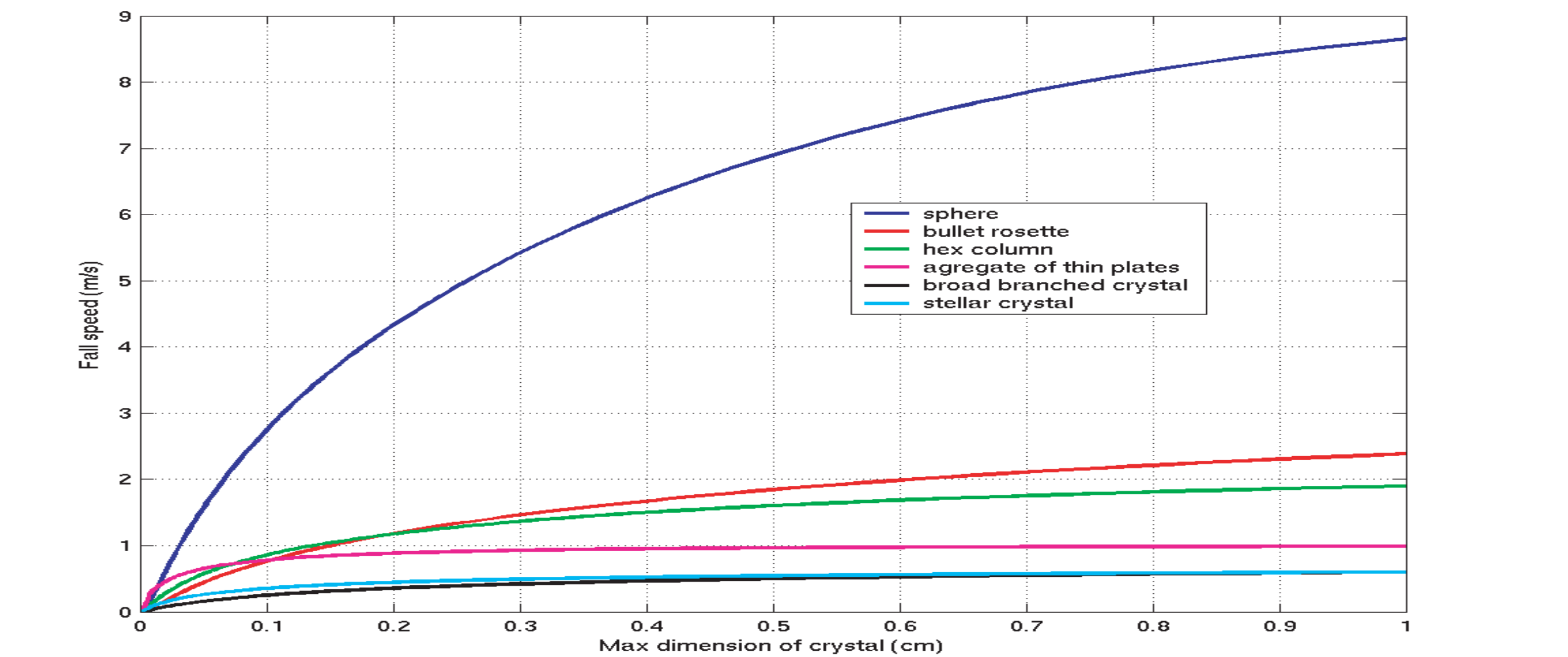


The circular depolarization measured between 13:00 and 16:00 on Sept 27. High depolarizations (red) indicate scattering from ice crystals while low depolarizations (blue) indicate that the optical scattering is dominated by scattering from spherical water droplets. Note that the minimum range observed by the radar is 200 m, thus it is not possible to make the flux computation below the water.

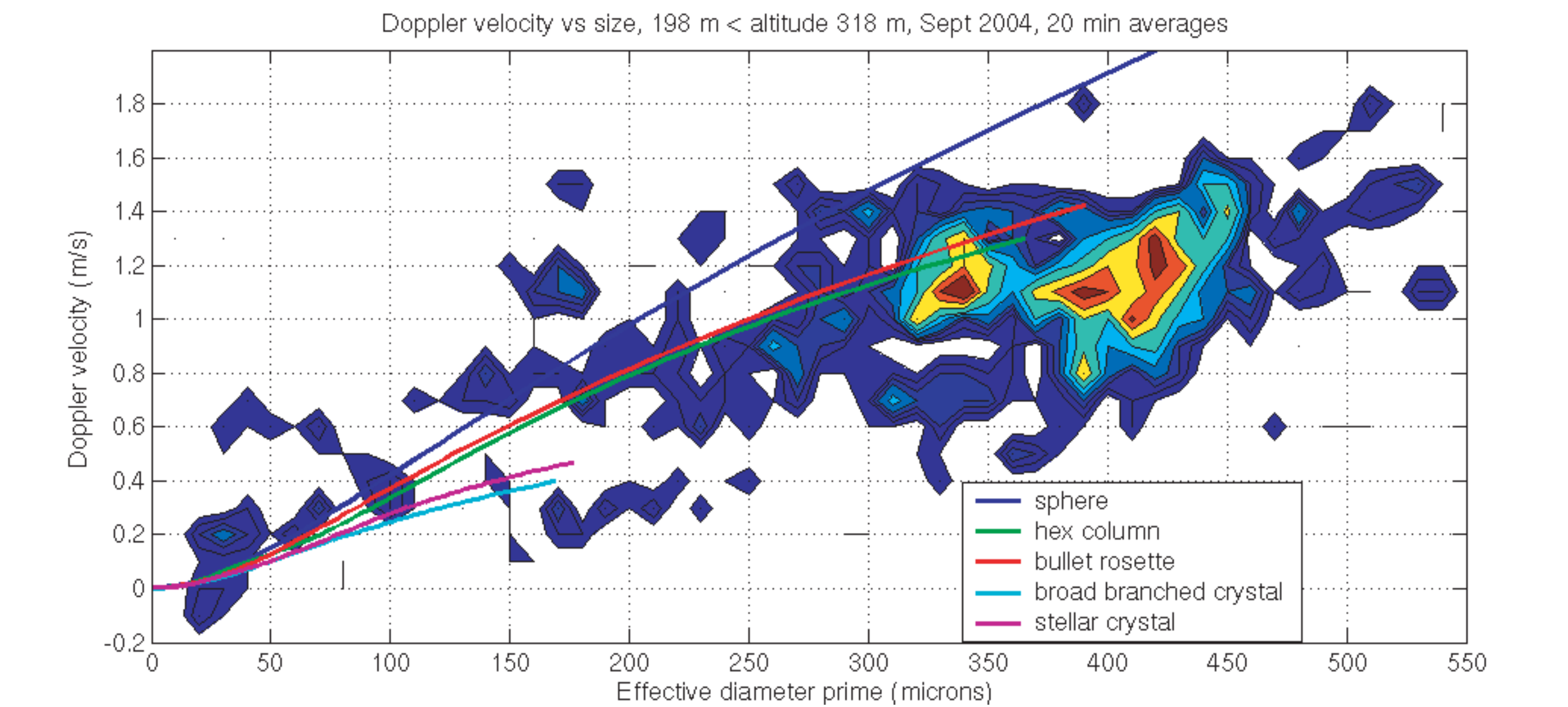


When the surface measurement of the accumulated precipitation (blue) is compared to the lidar-radar derived fluxes after 5:00 UT on 28-Sept, the measurement falls between the results derived for bullet rosettes and spheres. During this period, low level water clouds were not present in 250 m lidar and radar data used for the flux computations.

Fall velocity as a function of particle size is another potential means of distinguishing between ice crystal types. This plot shows particle fall velocities computed as a function of maximum dimension of the ice crystal (see Mitchell & Heymsfield, J Atmos. Sci, Vol 2, May 2005).



The number of occurrences of Doppler velocity at a given 'effective diameter prime' is plotted in the figure below. All data points at altitudes between 198 and 318 m are plotted for the period between 27-Sept. at 0 UT and 1-Oct at 0 UT. Each point consists of a 30 m altitude average. A 20 min time average was used to minimize the scatter produced by turbulent air motions. Also plotted are the fall velocities computed for several ice crystal types. Unfortunately, when the velocities are plotted vs effective diameter prime rather than the maximum dimension, the distinction between particle types decreases.



Acknowledgments: This research was funded by DOE grant DE-FG02-06ER64187